Supplementary Materials

Cell growth and mitochondrial anomalies in induced pluripotent stem cells with Presenilin 1 mutation

Rimi Hamam[1], Roy Hanna[1], Andrea Barabino[1], Dounya Serhani[1], Erika Tavares[2], Élise Héon[2], and Gilbert Bernier[1,3*]

[1] Stem Cell and Developmental Biology Laboratory, Hôpital Maisonneuve-Rosemont, 5690 Boul. Rosemont, Montréal, Canada, H1T 2H2

[2] Genetics and Genome Biology, The Hospital for Sick Children, Toronto, Canada

[3] Department of Neurosciences, Université of Montréal, Montréal, Canada

*Corresponding author

Tel: 514-252-3400 ext. 4648

E-mail: gbernier.hmr@ssss.gouv.qc.ca

Content:

Supplementary Material and Methods

6 supplementary figures and figures legends

Supplementary Material and Methods

Whole genome sequencing

Paired-end (2 x 150 bp) Whole Genome Sequencing (WGS) was performed using Illumina Hi-Seq X with mean coverage of 39.4 X for three affected (FAD24, FAD25, and FAD7) and three control samples (CTL1, CTL2, and CTL14), and Illumina NovaSeq 6003 with mean coverage 38.7% for two affected samples (FAD24, FAD25) and one control sample (CTL16). Base calling for the samples run in Illumina HiSeqX was performed using Illumina HiSeq Analysis Software (HAS; version 2-2.5.55.1311). Reads were mapped to the human b37 reference sequence using bwa-mem v0.7.12 [1]. Duplicate reads were removed using MarkDuplicates from Picard v2.5.0. Local read realignment around indels, base quality score recalibration (BQSR), variant calling with HaplotypeCaller, and variant quality score recalibration (VQSR) were accomplished using GATK v3.7.0 [2]. Illumina Dragen DNA platform version 3.8 was used for mapping reads to the human hg38 reference and for the base calling of samples FAD24, FAD25 and CTL16 (https://support-docs.illumina.com/SW/DRAGEN_v38/Content/SW/FrontPages/DRAGEN.htm).

Resulting variant calls were annotated using a custom pipeline developed at The Centre for Applied Genomics (TCAG) at SickKids based on ANNOVAR [3]. Structural variants were called using Manta v0.29.6 [4] and LUMPY v0.2.13 [5]. LUMPY calls were genotyped using SVTyper v0.1.2 [6]. Other protocols specific to copy number variants calling from WGS using read depth method were done by the programs ERDS v1.1 and CNVnator v0.3.2 using a window size of 500 bp [7, 8]. Variant prioritization was done on candidate genes for AD (Supplemental Figure X). Population frequency of candidate variants were verified on thousand genomes (1000g phase3;[9]) and Genome Aggregation Database v2.1.1 (gnomAD; [10]). Mutations and genotypes well known to cause AD in those genes were manually inspected from mapping file of affected and control samples on Integrative Genomic Viewer [11]. (TE), inversions and translocations. C) SpliceAI (https://github.com/Illumina/SpliceAI; [13]) was used to verify if mutations were likely to create an aberrant splicing event.

Supplementary References

1. Li, H. and R. Durbin, *Fast and accurate long-read alignment with Burrows-Wheeler transform.* Bioinformatics, 2010. **26**(5): p. 589-95.
2. McKenna, A., et al., *The Genome Analysis Toolkit: a MapReduce framework for analyzing next-generation DNA sequencing data.* Genome Res, 2010. **20**(9): p. 1297-303.
3. Wang, K., M. Li, and H. Hakonarson, *ANNOVAR: functional annotation of genetic variants from high-throughput sequencing data.* Nucleic Acids Res, 2010. **38**(16): p. e164.
4. Chen, X., et al., *Manta: rapid detection of structural variants and indels for germline and cancer sequencing applications.* Bioinformatics, 2016. **32**(8): p. 1220-2.
5. Layer, R.M., et al., *LUMPY: a probabilistic framework for structural variant discovery.* Genome Biol, 2014. **15**(6): p. R84.
6. Chiang, C., et al., *SpeedSeq: ultra-fast personal genome analysis and interpretation.* Nat Methods, 2015. **12**(10): p. 966-8.
7. Abyzov, A., et al., *CNVnator: an approach to discover, genotype, and characterize typical and atypical CNVs from family and population genome sequencing.* Genome Res, 2011. **21**(6): p. 974-84.
8. Zhu, M.F., et al., *Using ERDS to Infer Copy-Number Variants in High-Coverage Genomes.* American Journal of Human Genetics, 2012. **91**(3): p. 408-421.
9. Genomes Project, C., et al., *A global reference for human genetic variation.* Nature, 2015. **526**(7571): p. 68-74.
10. Karczewski, K.J., et al., *The mutational constraint spectrum quantified from variation in 141,456 humans.* Nature, 2020. **581**(7809): p. 434-443.
11. Robinson, J.T., et al., *Integrative genomics viewer.* Nat Biotechnol, 2011. **29**(1): p. 24-6.

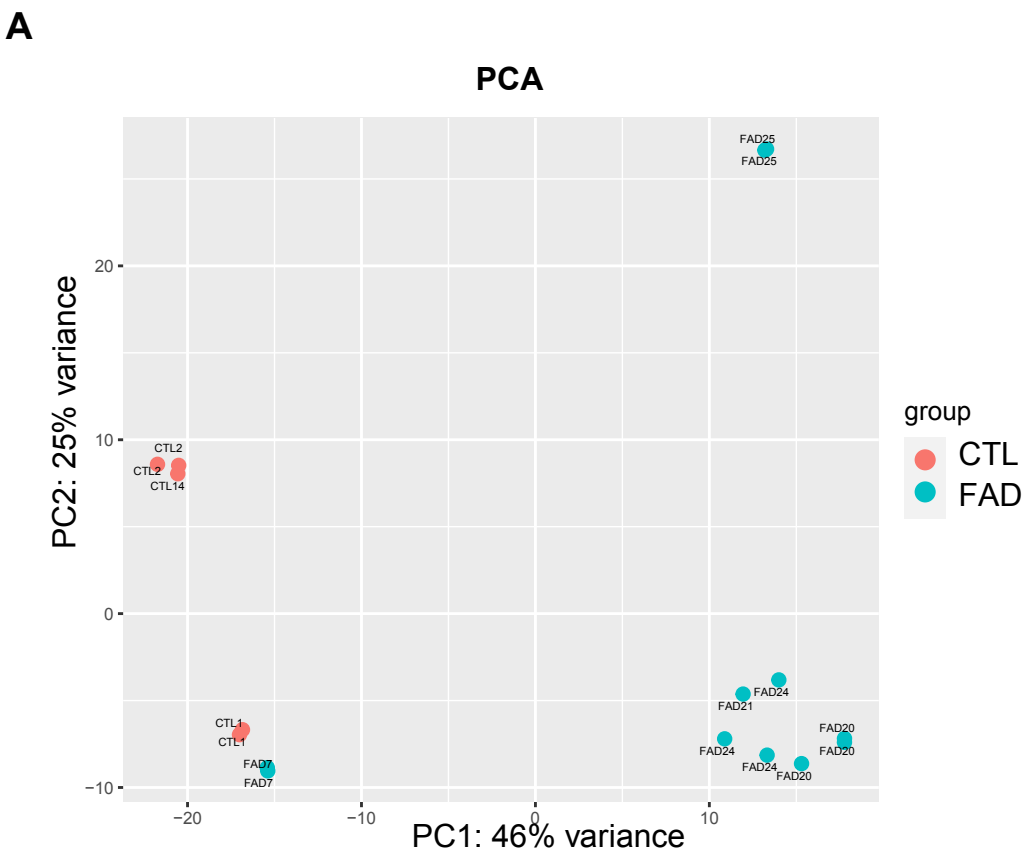
A
PCA
PC2: 25% variance
PC1: 46% variance
group
CTL
FAD
CTL2
CTL2
CTL14
CTL1
CTL1
FAD7
FAD7
FAD25
FAD25
FAD24
FAD21
FAD24
FAD24
FAD20
FAD20
FAD20

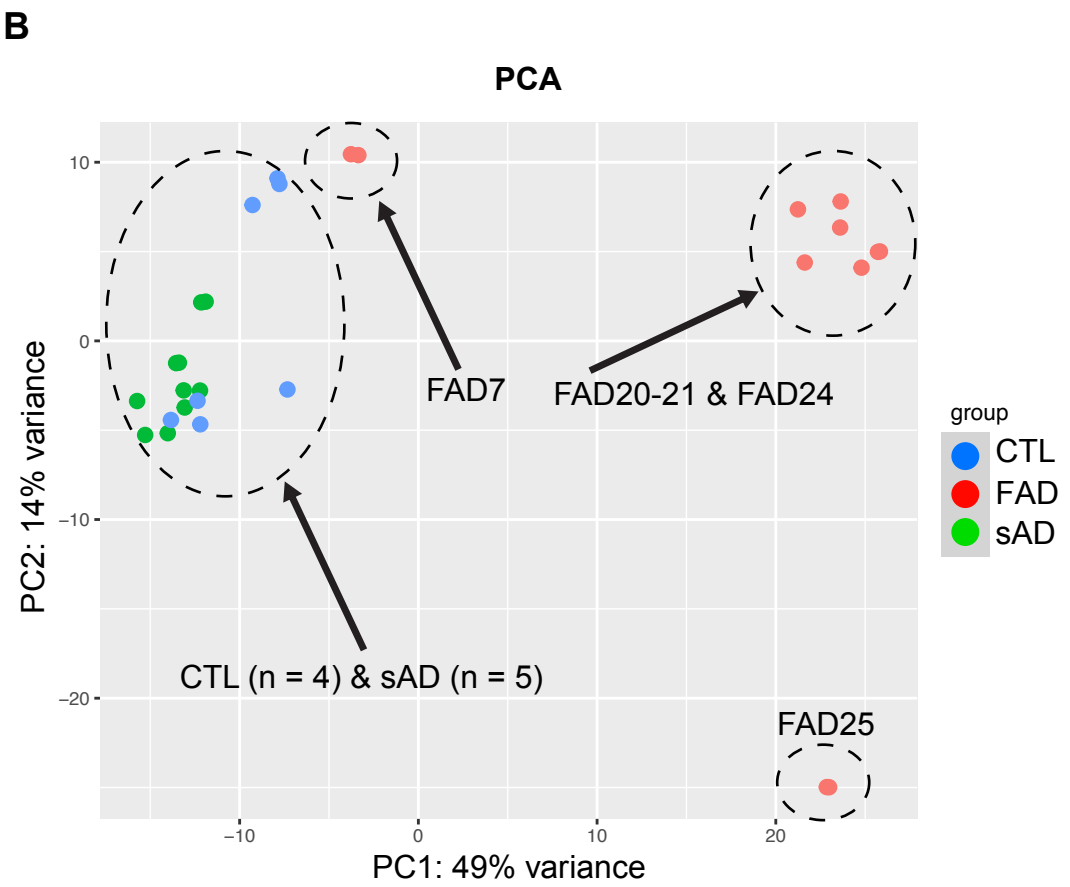
B
PCA
PC2: 14% variance
PC1: 49% variance
group
CTL
FAD
sAD
FAD7
FAD20-21 & FAD24
FAD25
CTL (n = 4) & sAD (n = 5)

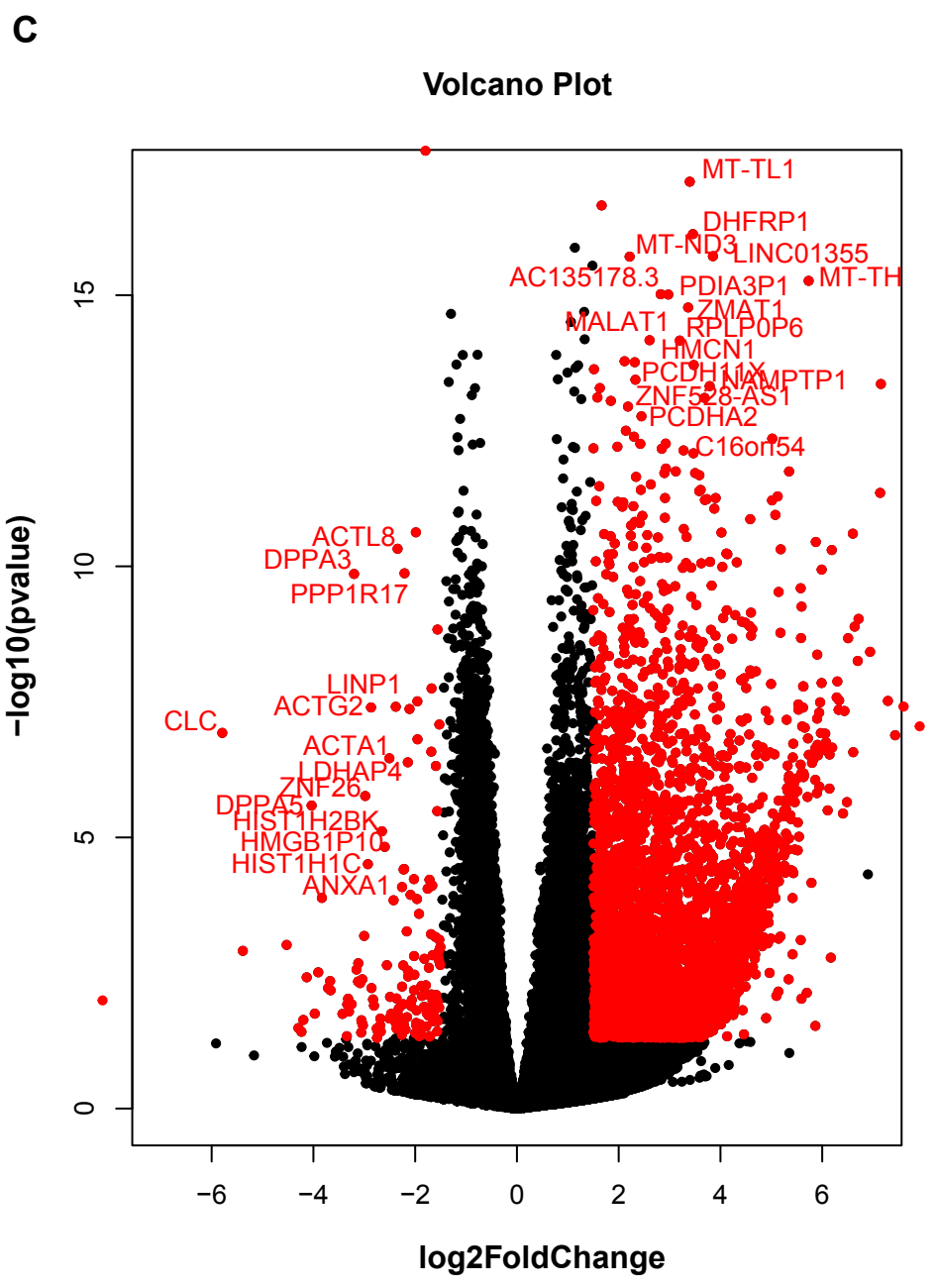
C
Volcano Plot
−log10(pvalue)
log2FoldChange
MT-TL1
DHFRP1
MT-ND3
LINC01355
AC135178.3
PDIA3P1
MT-TH
ZMAT1
MALAT1
RPLP0P6
HMCN1
PCDH11X
NAMPTP1
ZNF528-AS1
PCDHA2
C16orf54
ACTL8
DPPA3
PPP1R17
LINP1
ACTG2
CLC
ACTA1
LDHAP4
ZNF26
DPPA5
HIST1H2BK
HMGB1P10
HIST1H1C
ANXA1

Figure S1

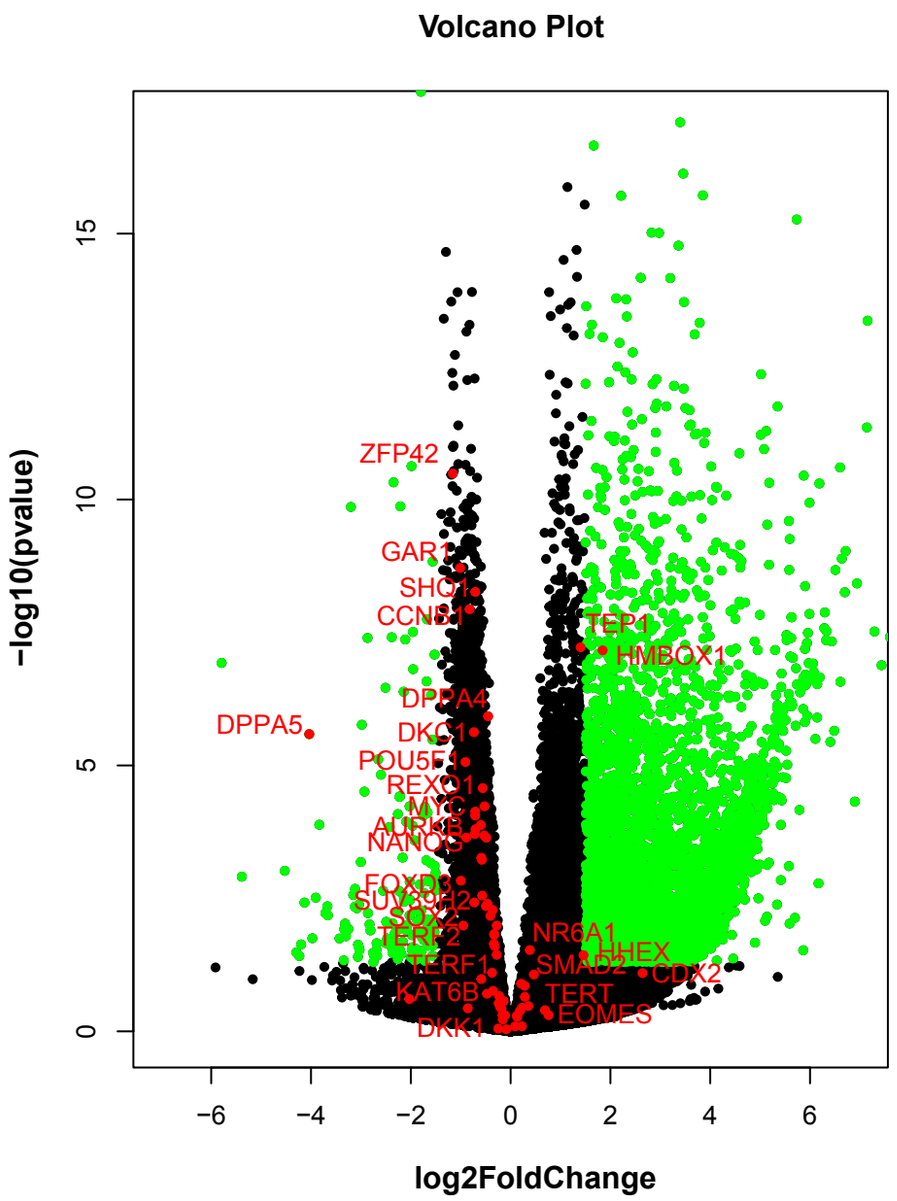
Volcano Plot
−log10(pvalue)
log2FoldChange
0
5
10
15
−6
−4
−2
0
2
4
6
ZFP42
GAR1
SHQ1
CCNB1
TEP1
HIMOX1
DPPA4
DPPA5
DKC1
POU5F1
REXO1
MYC
AURKB
NANOG
FOXD3
SUV39H2
SOX2
TERF2
TERF1
KAT6B
DKK1
NR6A1
HHEX
SMAD2
CDX2
TERT
EOMES

Figure S2

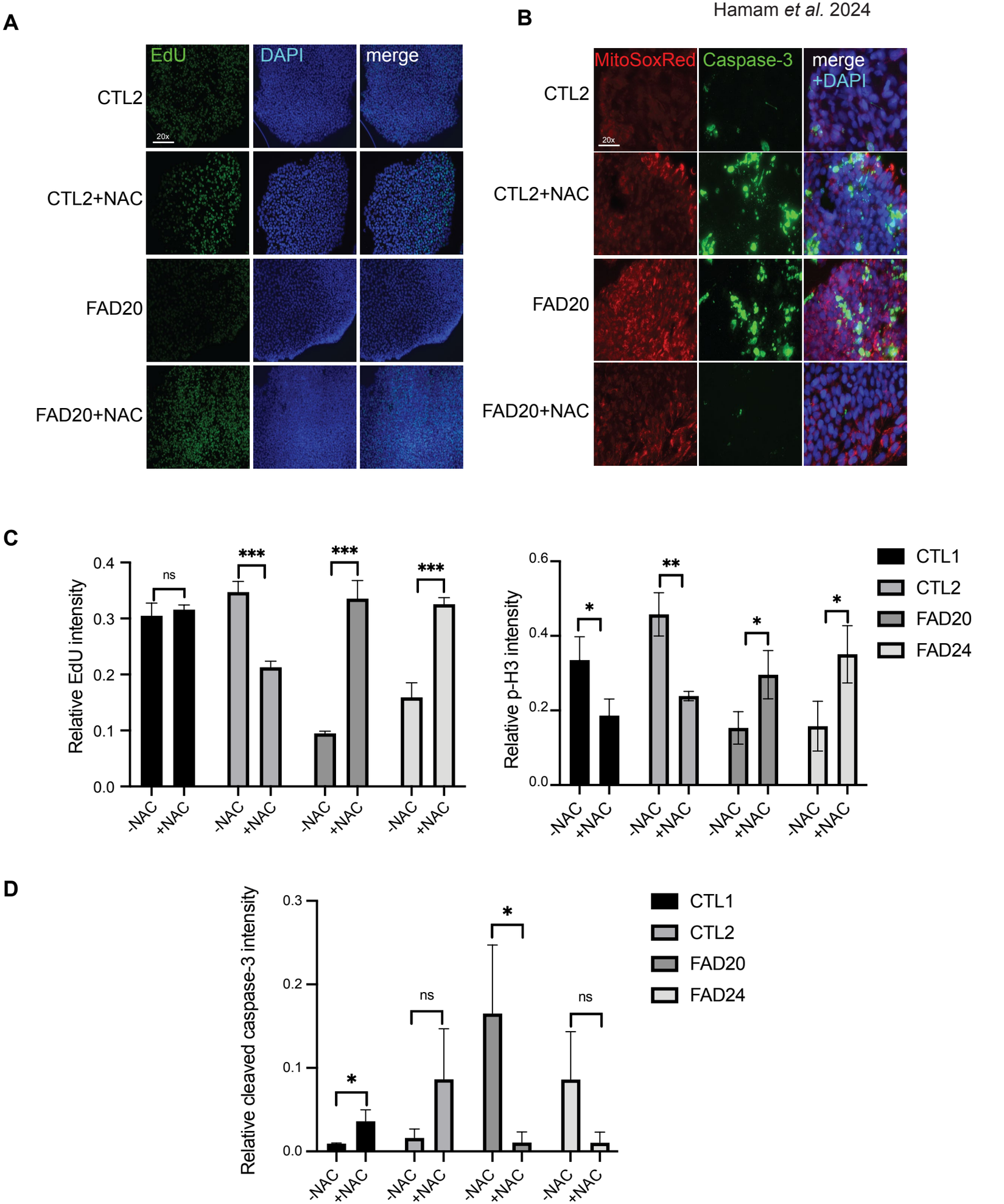
A
EdU
DAPI
merge
CTL2
CTL2+NAC
FAD20
FAD20+NAC
20x
B
MitoSoxRed
Caspase-3
merge +DAPI
C
Relative EdU intensity
Relative p-H3 intensity
ns
***
**
*
-NAC
+NAC
CTL1
CTL2
FAD20
FAD24
D
Relative cleaved caspase-3 intensity

Figure S3

A

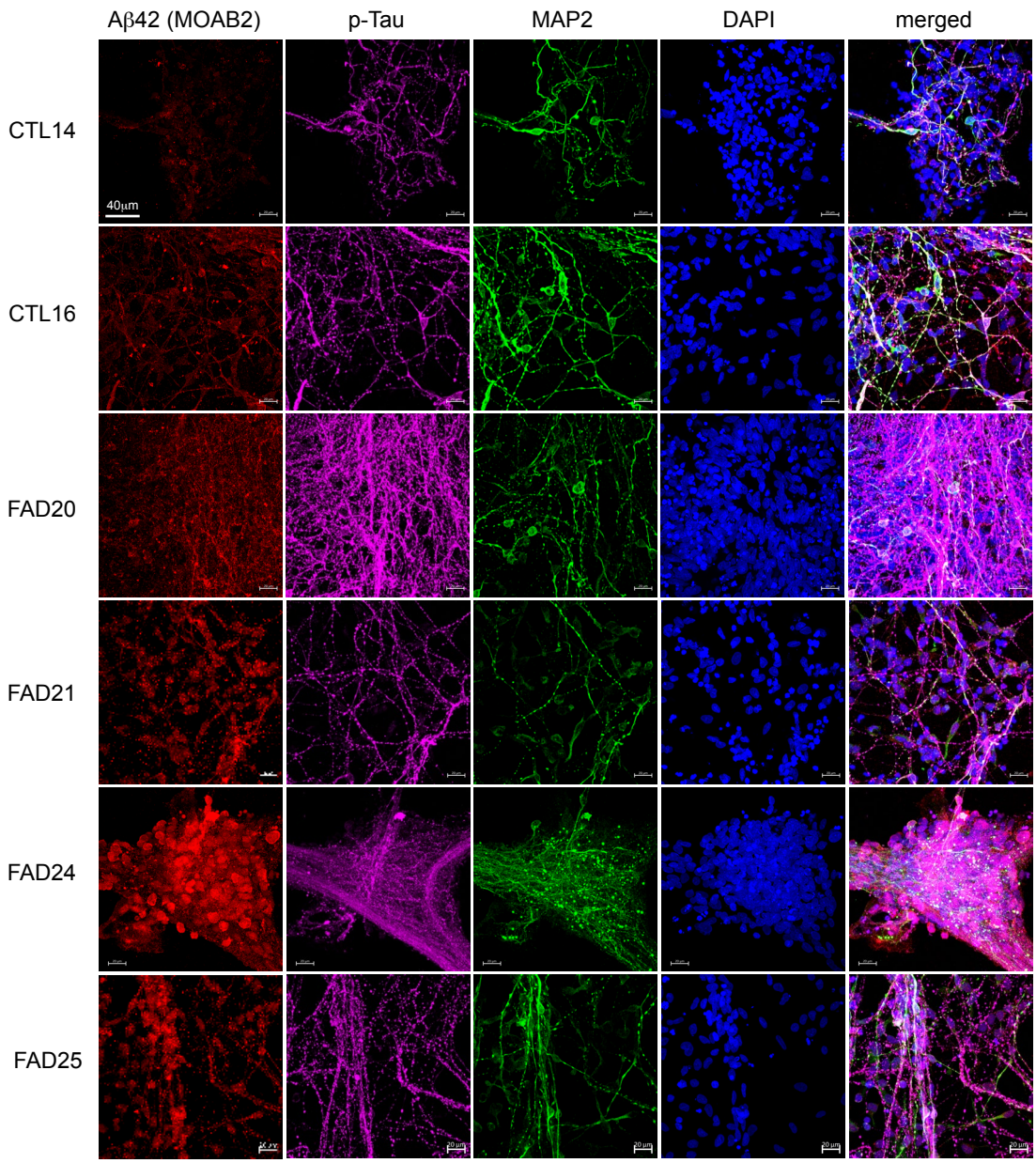
Aβ42 (MOAB2)
p-Tau
MAP2
DAPI
merged
CTL14
CTL16
FAD20
FAD21
FAD24
FAD25
40µm

B

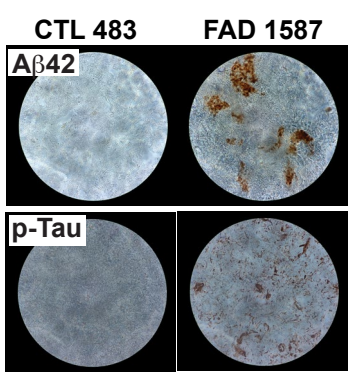
CTL 483
FAD 1587
Aβ42
p-Tau

Figure S4

A

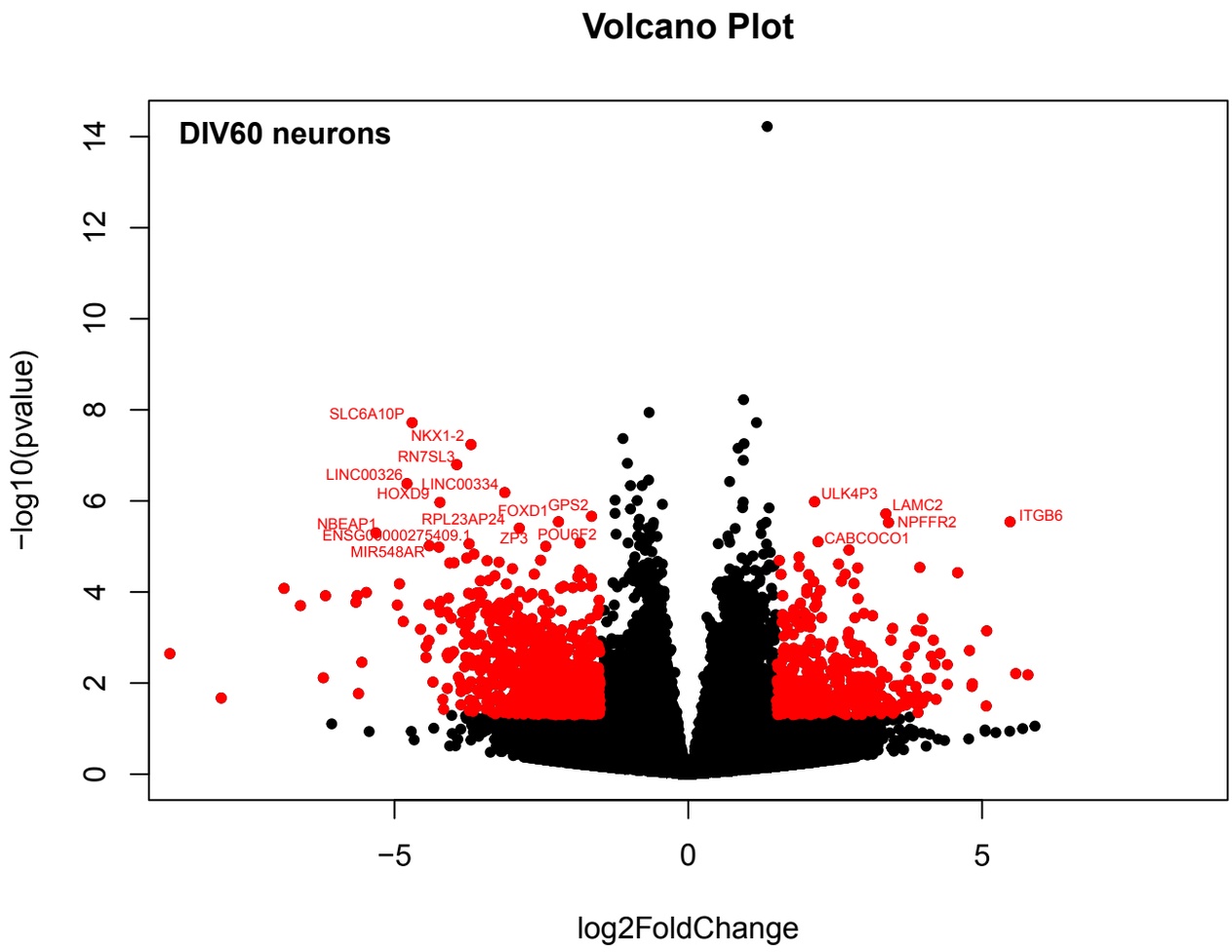
Volcano Plot
DIV60 neurons
−log10(pvalue)
log2FoldChange
SLC6A10P
NKX1-2
RN7SL3
LINC00326
LINC00334
HOXD9
FOXD1
GPS2
NBEAP1
RPL23AP24
ENSG00000275409.1
ZP3
POU6F2
MIR548AR
ULK4P3
LAMC2
NPFFR2
ITGB6
CABCOCO1

B

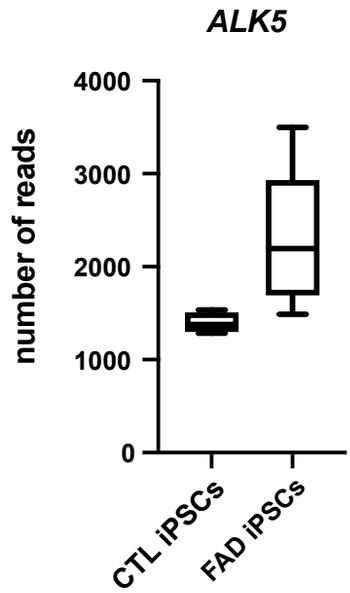
ALK5
number of reads
CTL iPSCs
FAD iPSCs

Figure S5

Supplementary Figure Legends

Figure S1. Gene expression analyses of CTL and FAD iPSCs

(A) Principal Component Analysis (PCA) plot of CTL and FAD iPSCs cell lines based on the expression levels of all genes in the dataset.

(B) Principal Component Analysis (PCA) plot of the CTL, FAD and sAD iPSCs cell lines based on the expression levels of all genes in the dataset. Note the segregation between the FAD group and the CTL and sAD groups (dot circles).

(C) Volcano plot depicting the most differentially expressed genes between CTL and FAD iPSC, with the x-axis indicating fold change (log2) and the y-axis representing statistical significance (-log10 p-value). A threshold of log fold change 1.5 was applied to highlight significant gene expression differences (in red).

Figure S2. Analysis of pluripotency genes in CTL and FAD iPSCs

Volcano plot analysis of 25 pluripotency genes (in red) between CTL and FAD iPSCs.

Figure S3. NAC treatment improves cell proliferation in FAD iPSCs

(A) EdU assay for CNT2 and FAD20 iPSCs. EdU staining (green) and DAPI staining (blue) show a reduction in cell proliferation in FAD iPSCs compared to the CTL iPSCs, which increased after the treatment with NAD (10 uM) for 24 hrs. CTL2 iPSCs show a reduction in proliferation upon NAC treatment.

(B) IF analysis showing accumulation of mitochondrial ROS in FAD iPSCs using MitoSox Red immunofluorescent staining (red), and normalization of ROS after treatment for 24 hours with NAC (10 uM) in the FAD iPSCs. Cleaved Caspase-3 labelling (green) in FAD20 iPSCs showed an increased level of cell death (arrowheads) in FAD iPSCs compared to CTL2, and a reduction in the apoptosis in FAD20 upon the treatment, where CTL2 showed induction of ROS and C-Caspase-3 after NAC treatment. Scale bars, 20 μm.

(C) Quantitative fluorescence intensity of accumulated Edu intensity comparing EdU-positive nuclei in each CTL (CTL 1 and CTL2) and FAD iPSCs (FAD20, FAD24 and FAD7) vs the same cell line treated with NAC. ns, not significant; $^{***}p < 0.0005$; $^{***}p < 0.0002$; $^{***}p < 0.0005$ and $^{***}p < 0.0006$, by Student's unpaired t-test. Quantification of p-H3 level in CTL (CTL1 and CTL2) and FAD iPSCs (FAD20, FAD24 and FAD7) w/wo NAC treatment. CTL cell line

proliferation was reduced after treatment with NAC, where the FAD iPSCs proliferation increased upon NAC treatment. *p <0.0280; **p < 0.0031; *p <0.0264; p <0.0306 and p* < 0. 0.302, by Student's unpaired t-test.

(D) Quantification of the IF results showing a decrease in cleaved Caspase-3 in FAD iPSCs (FAD20, FAD24 and FAD7) after treatment with NAC, where CNT (CTL and CTL2) showed an increase in cleaved Caspase-3 after treatment with NAC, *p <0.0268**;** ns, not significant; *p < 0.0320; ns, not significant and *p <0.0238, by Student's unpaired t-test, by Student's unpaired t-test.

Figure S4. Gene expression analysis of FAD neurons and iPSCs

(A) Immunofluorescence analysis of CTL and FAD neuronal cultures at DIV60.

(B) Immuno-histochemistry of CTL and FAD brain sections with anti-amyloid and anti-Tau antibodies. Positive signal is in brown color.

Figure S5. Gene expression analysis of FAD neurons and iPSCs

(A) Volcano plot depicting the most differentially expressed genes between CTL and FAD DIV60 neuronal cultures, with the x-axis indicating fold change (log2) and the y-axis representing statistical significance (-log10 p-value). A threshold of log fold change 1.5 was applied to highlight significant gene expression differences (in red).

(B) Expression levels of *ALK5* in CTL and FAD iPSCs as measured by RNA-seq analysis.

Legend for the original blots

Uncropped full-length pictures of western blotting membranes.
Uncropped full-length images of Western blotting membranes presented in Figure 6B and Figure 7C and G.
Membranes were often cut to enable blotting with multiple antibodies.

Figure 6 B

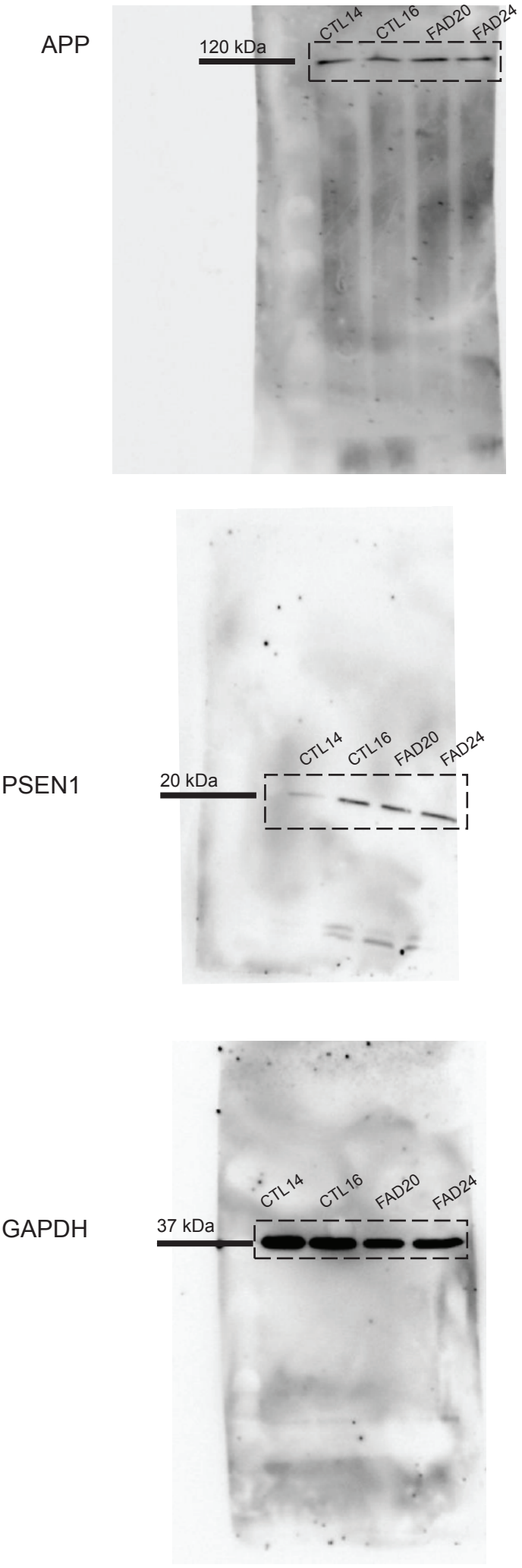
APP
120 kDa
CTL14
CTL16
FAD20
FAD24
PSEN1
20 kDa
CTL14
CTL16
FAD20
FAD24
GAPDH
37 kDa
CTL14
CTL16
FAD20
FAD24

Figure 7 C

Total Tau
(A0024)

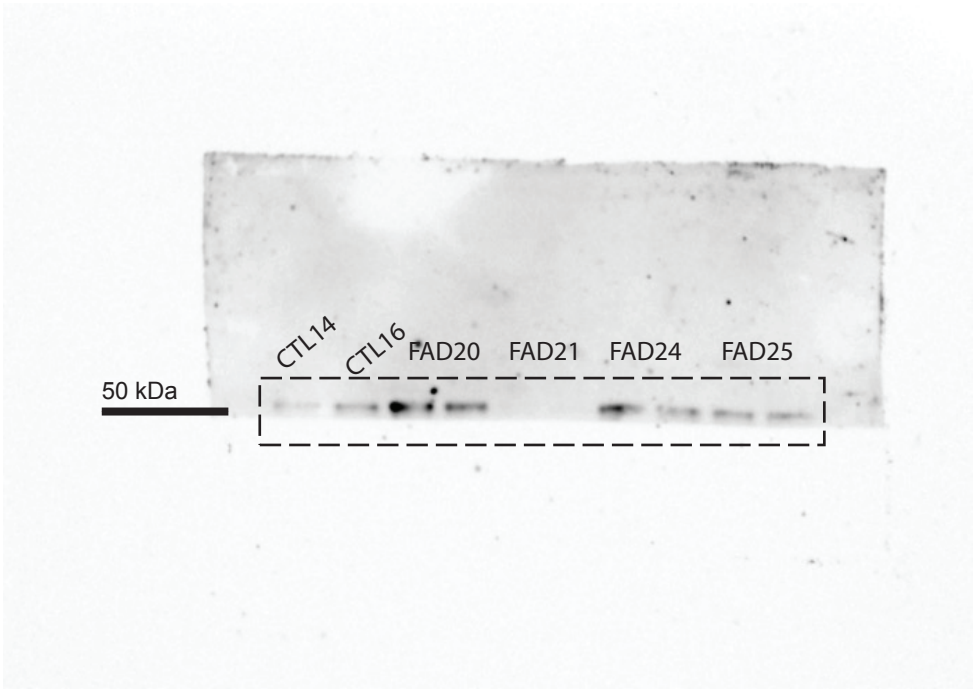

p-Tau
(ser396)

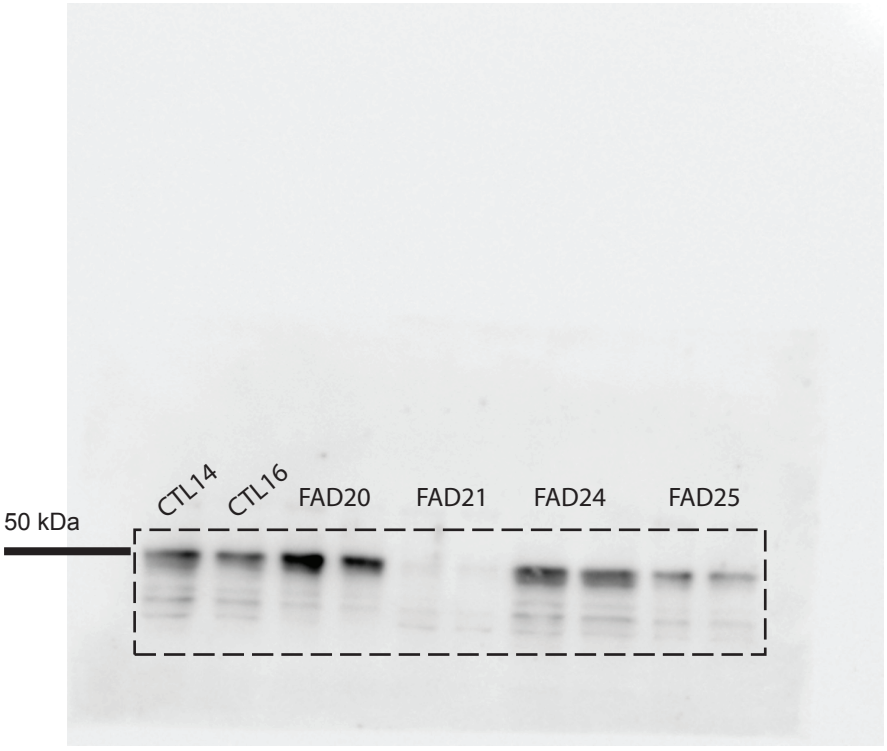

β-actin

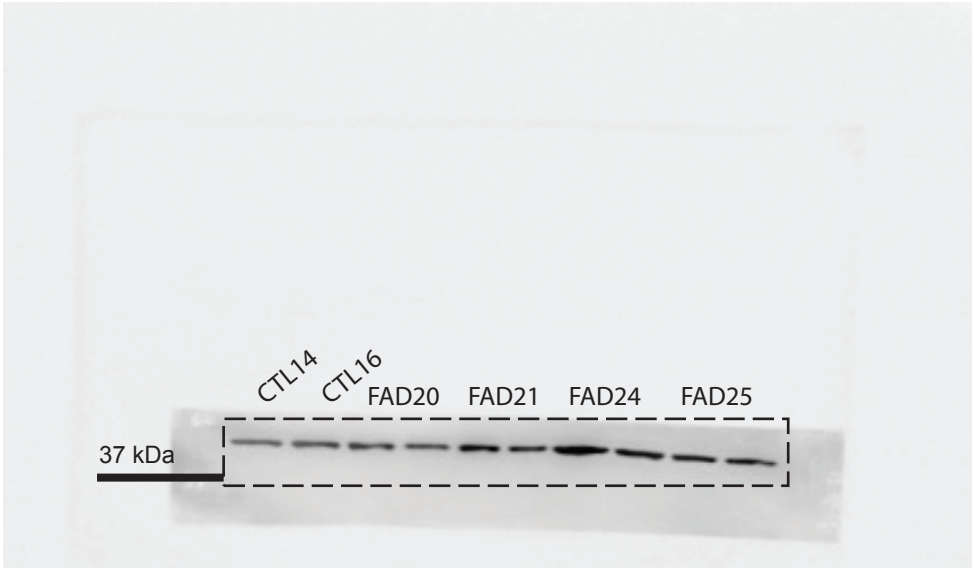

Figure 7 G

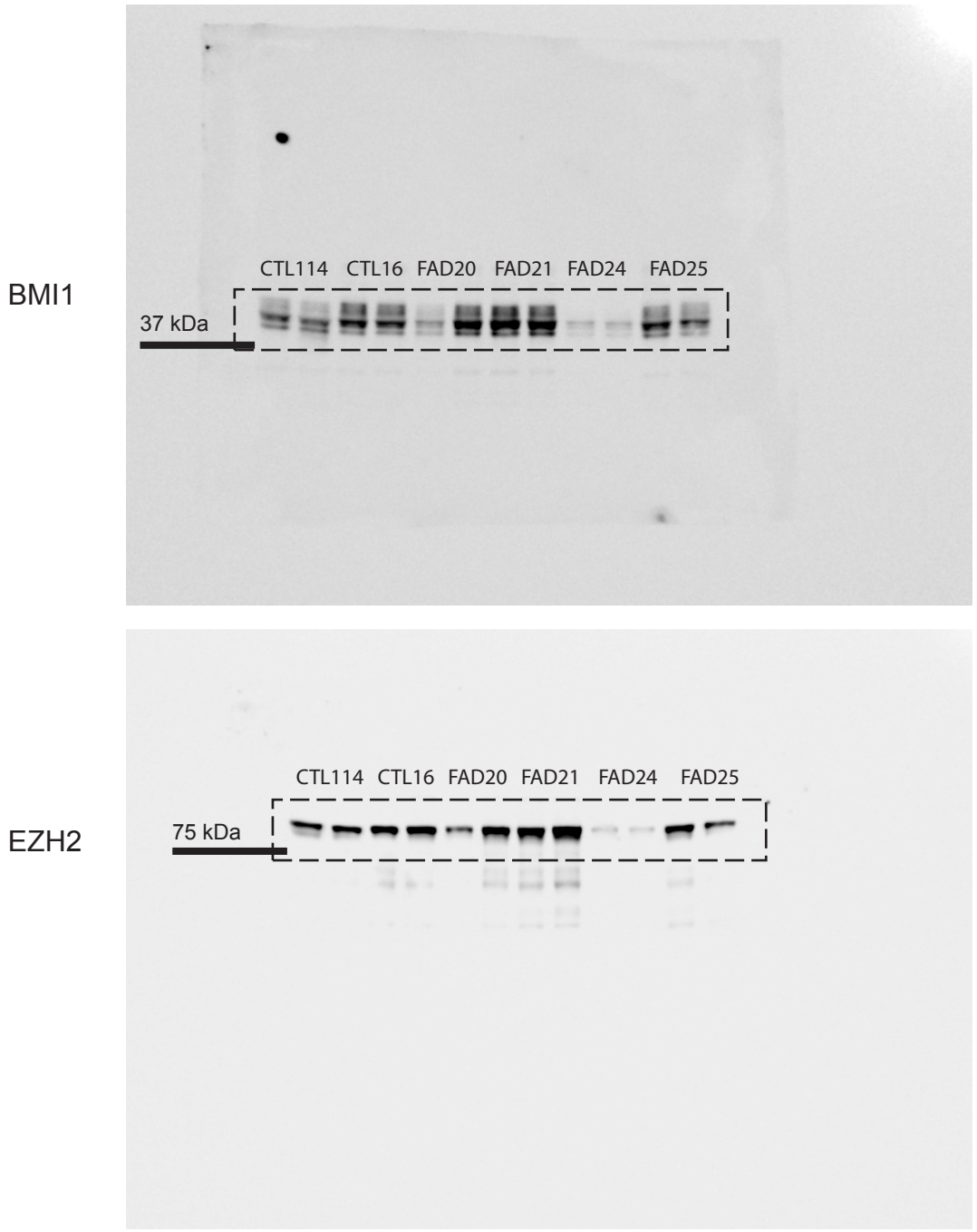
BMI1
CTL114 CTL16 FAD20 FAD21 FAD24 FAD25
37 kDa
EZH2
CTL114 CTL16 FAD20 FAD21 FAD24 FAD25
75 kDa
GAPDH
CTL114 CTL16 FAD20 FAD21 FAD24 FAD25
37 kDa